Intern. J. Pavement Engineering, 2000, Vol. 1(2), pp. 133-149
Reprints available directly from the publisher
Photocopying permitted by license only

A Model for Fatigue Cracking Prediction of Asphalt Pavements Based on Mixture Bonding Energy

RÉGIS MARTINS RODRIGUES*

Assistant Professor Instituto Tecnológico de Aeronáutica – ITA Divisão de Engenharia de Infra-Estrutura Aeronáutica – IEI São José dos Campos – SP – BRASIL CEP: 12.228–900

(Received August 25, 1998; Revised August 10, 1999)

The problem of fatigue cracking prediction on asphalt concrete pavements under the action of repeated loads is addressed through a model that is based on damage analysis performed from the point of view of a gradual loss of the bonding energy existing on the asphalt concrete mixture. A model was thus developed that could take into account several factors affecting cracking behaviour on pavement structures that were not considered adequately up to now, such as traffic speed and the shape of the stress pulse. This model describes the process that leads to fatigue cracks appearance at the pavement surface on the basis of a single mechanism, without the need to calculate stress intensity factors for the analysis of crack propagation through the thickness of the asphalt concrete layer. Application of the model to experiments at Nantes circular test track showed promising results.

Keywords: Asphalt pavements, Fatigue cracking, Performance prediction, Asphalt concrete mixtures

INTRODUCTION

A reliable prediction model for fatigue cracking of asphalt concrete surface layers under traffic loads is a key tool for pavement structural design and for specification of asphalt concrete mixtures, if the most efficient use of available resources is to be made. There is not at present a model capable to take into account all main factors known to affect fatigue performance of the asphalt concrete layer on the pavement structure. Material variability can be successfully incorporated for assessment of design reliability only if the physical model employed for performance predictions is consistent with behaviour observed on tests performed under controlled and known conditions. In this way, fracture behaviour of asphalt concrete is here analysed from fundamental considerations in order to develop a model that could reproduce laboratory fatigue and accelerated field-tests results.

Fatigue cracking under repeated loads has been described as a two-stage process: crack formation followed by crack progression. Laboratory phenomenological models that relate the number of load cycles up to crack formation to amplitude of the stress or strain pulse applied describe the first stage, and the second one is accounted for by calibration factors or by prediction models developed from linear elastic fracture mechanics principles. Several experimental

* Correspondence Author: Tel: (+55 12) 347–6804 Fax: (+55 12) 333–2611 e-mail: regis@infra.ita.cta.br

studies have shown the validity of fracture mechanics concepts when applied to asphalt concrete (Molenaar 1984, Majidzadeh and Ramsamooj 1973). In this way, there would be a number of load cycles N_0 required for fatigue fracture, when a macroscopic crack appears at the critical stressed zone, and an additional number of load cycles ΔN would be required to drive the crack to a certain length. This separation in two stages may be, however, fictitious, since there are microcracks in every material and fatigue fracture could be viewed as the result of a complex process where these micro-cracks grow and join themselves (coalesce) leading to a macroscopic crack. On the other hand, fracture mechanics concepts (stress intensity factors, Paris' law) have difficulties when dealing with such microscopic cracks. These principles are easily applied only to the second stage, with ΔN being calculated supposing a sharp crack with stress field at the crack tip described by the stress intensity factor. Besides, initial construction voids can also be the source of propagating cracks, if these voids are able to concentrate stresses and if it is possible for them to follow a path where energy is dissipated at the crack tip to form free surfaces. The irregular path followed by a crack that goes around aggregate particles arises doubts, however, as to the relevance of stress intensity factors calculations on this so heterogeneous material. In fact, asphalt concrete is a granular material where grain particles are held on their original positions inside the aggregate matrix by cohesion given by the bituminous mastic and by aggregate interlock. This configuration is in contradiction with continuum mechanics hypotheses on which stress intensity factors calculations are based.

Rowe (1993) observed on fatigue tests conducted at controlled strain that stiffness of the cantilever beam tested fell to 50 % of its original value without any visible sign of a crack at the beam. Since the beginning of fatigue tests, there is a continuous decrease on the stiffness of the tested specimen. This decrease could be interpreted as the result of growth of micro-cracks, or of a gradual cohesion reduction of the mix under repeated loads. This last hypothesis is worth to investigate due to the granular nature of the material, where fatigue fracture would be viewed as a continuous breakdown of bonds at the particle points of contact.

According to Hertzberg (1989): "Materials possess low fracture strengths relative to their theoretical capacity because most materials deform plastically at much lower stress levels and eventually fail by an accumulation of this irreversible damage. In addition, materials contain defects that are micro-structural in origin or introduced during the manufacturing process". Failure is, therefore, the final result of irreversible changes of a micro-structural character that lead to cohesion loss of the material. One way to deal with these deformations is to see them as a result of discrete jumps of certain flow units under the action of shear or tensile stresses. These flow units jump between adjacent equilibrium positions defined by material imperfections. According to Abdel-Hady and Herrin (1966), the "absolute rate theory", which was originally a theory of kinetics of chemical reactions, can be applied to any process involving the rearrangement of matter. Mitchell (1976) applied the theory of rate processes to describe strength and deformation behaviour of soils and showed that an estimate of the number of inter-particle bonds with the help of this theory was able to explain shear strength in fundamental concepts. In this way, the onset of fatigue fracture could be viewed as the result of loss of stability at the stressed point when accumulation of microscopic changes generated by the applied stresses exhausts the bonding energy of the material.

Tensile or shear stresses at failure are not fundamental parameters of a material, since their values depend on mode of load application, stress state and strain rate. Rupture along a certain plane could be viewed as the result of the breaking of bonds at a surface oriented according to the reference plane but curved in order to intercept grain boundaries and inter-particle contacts. Failure would be the result of energy dissipated in the process of breaking all the bonds existing on the reference surface. Thus, to open a crack on a certain point would be equivalent to exhaust total bonding energy stored along the plane where the crack is to be formed at that point. In fact, Tayebali *et al.* (1993) could express fatigue life on controlled strain tests by the model:

$$N_f = 466.4e^{0.0521VFA}\varepsilon_0^{-3.948}(E_0'')^{-2.270} \quad (1)$$

where:

$E_0'' = E_0 \sin\phi$ = loss modulus (psi);
E_0 = initial flexural stiffness (psi);
ϕ = phase angle between stress and strain;
ε_0 = strain amplitude;
VFA = voids filled with asphalt (%).

The loss modulus is related to the initial energy dissipated per cycle (w_0) by:

$$w_0 = \pi\varepsilon_0^2 E_0 sin\phi_0 \quad (2)$$

where ϕ_0 is the initial phase angle. This expression for dissipated energy is valid always when, under a sinusoidal applied stress, the resulting strain is also sinusoidal, such as in the case of viscoelastic materials. In the same way, Rowe (1993) could express fatigue life by a model dependent upon w_0 and by the "work ratio", defined as the relation between w_0N_f and cumulative dissipated energy during the fatigue test. These results indicate that the process of energy dissipation during the test must be controlling fatigue fracture.

An alternate form of fatigue description is the use of linear elastic fracture mechanics and Paris' law:

$$\frac{dc}{dN} = AK_1^n \quad (3)$$

where the stress intensity factor K_I is given, for the simple case of a plate under tensile stress σ:

$$K_1 = \sigma\sqrt{\frac{\pi}{2}c} \quad (4)$$

Use of this approach for fatigue cracking prediction requires that a sharp crack exists or has been formed and that crack progression will monopolize the dissipated energy on the material, employing it for its extension under repeated loads. This must be true once such a crack exists and this has been the procedure adopted for fatigue analysis of metallic structures, where linear elastic fracture mechanics principles proved to be valid. For asphalt concrete this approach was also proved to be applicable but there remains the question of predicting the number of load cycles until a sharp stress concentrating crack has been formed, in order that Paris law becomes applicable. If N_0 is this number and c_0 is the minimum crack length required for Paris' law applicability, the result of a stress controlled fatigue test would be given by:

$$\int_{c_0}^{c_c} c^{-\frac{n}{2}}dc = \int_{N_0}^{N_c} A\sigma^n \left(\frac{\pi}{2}\right)^{\frac{n}{2}} dN \quad (5)$$

$$N_c = N_0 + \left(\frac{2}{\pi}\right)^{\frac{n}{2}} \frac{c_c^{\left(1-\frac{n}{2}\right)} - c_0^{\left(1-\frac{n}{2}\right)}}{A\left(1-\frac{n}{2}\right)} \left(\frac{1}{\sigma}\right)^n \quad (6)$$

where c_c is the critical crack length for instability, reached after N_c load cycles. Considering that stress controlled tests on asphalt concrete usually end at the moment when a crack becomes visible and that this moment is the one here described by N_0:

$$N_0 = K_{TC}\left(\frac{1}{\sigma}\right)^n \quad (7)$$

results:

$$N_c = \left[K_{TC} + \left(\frac{2}{\pi}\right)^{\frac{n}{2}} \frac{c_c^{\left(1-\frac{n}{2}\right)} - c_0^{\left(1-\frac{n}{2}\right)}}{A\left(1-\frac{n}{2}\right)}\right] \left(\frac{1}{\sigma}\right)^n \quad (8)$$

which is an equation that can be used to analyse fatigue test results, if crack length is registered during the test and if c_0 can be determined with accuracy. For laboratory determination of Paris' law parameters *A* and *n* it is advisable to employ pre-cracked specimens in order that crack progression can be measured. Use of equation 8 implies, therefore, a two step analysis: fracture formation on the material (N_0) and subsequent crack growth under Paris' law.

If it is desirable to adopt a terminal pavement condition for fatigue design associated with a certain degree of surface cracking (10 to 30 % of area cracked, for example), Paris' law can be applied for analysis of horizontal crack progression after a vertical crack is passing through the entire layer thickness. For progression under bending mode, Folias' (1970) solution can be employed (K_I), complemented by another one for the tearing mode (K_{III}). Consideration of this additional life seems important, since the post-crack behaviour of an asphalt concrete mixture with rough and coarse aggregates will be superior in comparison to a sand-asphalt mixture, for example, due to aggregate interlocking at the crack walls, which will reduce stress intensity factors on the coarser mixture. However, for prediction of the crack appearance at the pavement surface, use of equation 8 is problematical, since it is difficult to determine c_0. Besides, when the fracture mechanics approach is employed, analysis considers energy dissipation only at the tip of an idealized crack, while every point on the asphalt concrete layer is being subjected to tensile and/or shear stresses that are able to produce energy dissipation associated with loss of cohesion on the material. That was the basic motivation of the present study.

THEORETICAL MODELLING

Consider the case of a tensile creep test on asphalt concrete. Stiffness modulus measured on the test can be given by:

$$S = \frac{\sigma}{\varepsilon(t)} = \alpha \times t^{-m} \tag{9}$$

where σ is the applied tensile stress and α and m are material and temperature dependent parameters. Under this functional relation, the strain rate is given by:

$$\frac{\partial \varepsilon}{\partial t} = \frac{\sigma}{\alpha} m t^{m-1} \tag{10}$$

The external work per unit volume done at the test specimen up to tensile failure at time t_f is, therefore:

$$\begin{aligned} W_e = U + W_{R0} &= \sigma \int_0^{t_f} \frac{\partial \varepsilon}{\partial t} dt \\ &= \frac{1}{2}\sigma\varepsilon_E + \sigma \int_{t_0}^{t_f} \frac{\partial \varepsilon}{\partial t} dt \end{aligned} \tag{11}$$

where U is the elastic potential energy, stored due to development of elastic strain ε_E. The second term (W_{R0}) is the bonding energy per volume of the asphalt concrete mix, associated with the strains that develop after the elastic strain and from time t_0 to time t_f. It is implicit on equation 11 that all dissipative processes are responsible for failure and are enclosed under term W_{R0}, which can be calculated by:

$$W_{R0} = \sigma \int_{t_0}^{t_f} \frac{\sigma}{\alpha} m t^{m-1} dt = \frac{\sigma^2}{\alpha}(t_f^m - t_0^m) \tag{12}$$

Since t_0 (the time for the complete development of elastic strains) depends upon inertial effects, which are negligible on a small test specimen, t_0 can be neglected to write:

$$W_{R0} \approx \frac{\sigma^2}{\alpha} t_f^m \tag{13}$$

The fatigue life on a stress controlled test can be expressed by equation 7 with $N_f = N_0$. If fatigue failure is considered to be the result of irreversible transformations on the material that happen during all the time the stress σ is actuating, the fatigue life under repeated loads could be approximately predicted from creep tests writing:

$$N_f = \frac{t_f}{\Delta t_c} \tag{14}$$

where Δt_c is the time duration of the stress pulse σ. In fact, Phadnavis and Swaminathan (1977) could predict repeated load fatigue life of an asphalt concrete mixture from creep or from constant strain rate tests by an analogous procedure, assuming that accumulated plastic strain up to failure is a material constant, independent of the mode of loading. Combining equations 7, 13 and 14:

$$W_{R0} \approx \frac{(\Delta t_c K_{TC})^m}{\alpha} \sigma^{2-n\times m} \tag{15}$$

and a condition required for W_{R0} to be considered a fundamental material parameter (and, therefore, insensitive to applied stress) is that:

$$n = \frac{2}{m} \tag{16}$$

Jayawickrama and Lytton (1987) reported that this relation was deduced by Schapery (1981) for nonlinear viscoelastic composite materials and was verified to be applicable to asphalt concrete by Germann and Lytton (1979) and by Molenaar (1983). It can be concluded, therefore, that there exists a parameter W_{R0} that is fundamental in terms of failure prediction, and that this parameter is related to the dissipative processes that cause irreversible changes on the material. Parameter n, on the other hand, is not a constant, as is usually implied when "general" fatigue relations of the type:

$$N_f = K\left(\frac{1}{\varepsilon}\right)^n \tag{17}$$

are employed. From equation 16, it is clear that n must decrease with a temperature increase, since mixture stiffness becomes more sensitive to time of loading (so that m increases). The importance of not to consider parameter n a fixed one is readily apparent at correlations of the type:

$$n = -0.1093 \log_e K + 1.4749 \qquad (18)$$

developed from a total of 89 fatigue lines (Figure 1) at controlled stress tests presented by Bonnaure et al. (1980), Maupin and Freeman (1976), Tangella et al. (1990) and others (Table I).

Taking into consideration these suggestions, total bonding energy that is stored on a material and that must be extracted in order that a crack can appear along a certain plane will be considered here a fundamental material property. Designating this parameter by W_{R0}, its determination from fatigue tests can be made by the formula:

$$W_{R0} = -\int_0^{N_f} \frac{dW_R}{dN} dN \qquad (19)$$

Cohesion loss per load cycle, here expressed as loss of bonding energy per load cycle (dW_R/dN), involves

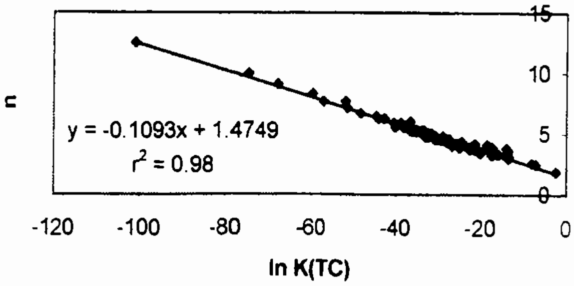

FIGURE 1 Controlled stress fatigue tests

only a fraction of the total dissipated energy, since there are also heat generation and other more complex mechanisms of energy dissipation, including plastic strains not associated necessarily with loss of cohesion. In order to get an initial reference, consider the simple rheological models of Maxwell or Kelvin (Figures 2 and 3) where the rate of dissipated energy is given by:

$$\frac{dW_D}{dt} = \sigma \frac{d\varepsilon_V}{dt} = \frac{1}{\eta}\sigma^2 \qquad (20)$$

TABLE I Controlled stress fatigue test results (mainly from third-point flexure and rotating flexure tests)

Asphalt Mixture	*K*	*n*	*Source*
Vitginia (AC-20)	2.8×10^{-8}	3.9	
Virginia (50–69 pen.)	2.7×10^{-4}	2.6	
Vitginia (120–150 pen.)	8.5×10^{-2}	1.9	Maupin and Freeman
Pennsylvania	1.0×10^{-6}	3.6	(1976)
Ohio	7.0×10^{-4}	2.5	
Utah	9.5×10^{-9}	4.1	
California	6.4×10^{-7}	3.8	
Monismith *et al.*, 1977	4.68×10^{-10}	3.73	
Saal and Pell, 1960	1.44×10^{-16}	6.00	Tangella *et al.* (1990)
Pell and Taylor, 1969	1.74×10^{-14}	4.91	
T = 40°F	9.67×10^{-7}	2.97	
T = 68°F	8.35×10^{-12}	4.17	
V_B = 12%, V_V = 4%,	1.026×10^{-7}	3.29	The Asphalt Institute
$\lvert E^* \rvert$ = 4000 MPa			(MS-1, 1981)
75 mixes/test conditions	varied	varied	Bonnaure *et al.* (1980)
T = 20°C, M_R = 5100 MPa	4.02×10^{-20}	6.43	OCDE (1991)

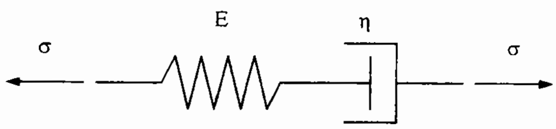

FIGURE 2 The Maxwell model

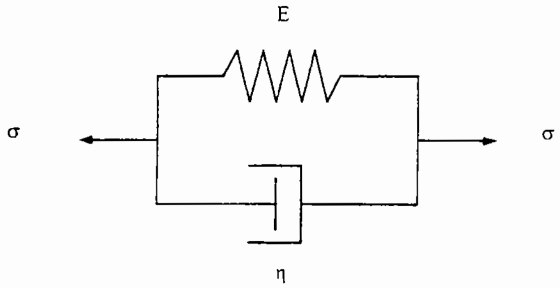

FIGURE 3 The Kelvin model

In this case, the rate of viscous strain ($d\varepsilon_V$-dt) is proportional to applied stress (σ) through viscosity coefficient (η). On the Maxwell model, if applied to asphalt concrete, elastic modulus E would be responsible for behaviour at small strains and at short loading times, while the viscous term would account for the plastic flow at grain boundaries responsible for the time-dependent strain. Equation 20 becomes, under a sinusoidal stress pulse $\sigma(t) = \sigma_0 \sin\omega t$:

$$\frac{dW_D}{dt} = \omega \frac{\sin\phi}{|E^*|}\sigma^2(t) \quad (21)$$

for the Maxwell model, and:

$$\frac{dW_D}{dt} = \frac{\omega}{|E^*|\sin\phi}\sigma^2(t) \quad (22)$$

for the Kelvin model, where $|E^*|$ is the dynamic modulus. Since viscous flow is a thermally activated process, application of the theory of rate processes (Mitchell, 1976) leads to:

$$\frac{d\varepsilon_V}{dt} = Ce^{\left(\frac{-\Delta F}{RT}\right)}\sigma \quad (23)$$

for Newtonian fluids, where:

ΔF = activation energy (J/mol)
T = absolute temperature (K)
R = universal gas constant = 8.312 J/K
C = a material parameter

Equation 23 leads, for the Maxwell model, to:

$$\sin\phi = a_0 \left(\frac{|E^*|}{\omega}\right)^{a_1} e^{\left(\frac{-\Delta F}{RT}\right)} \quad (24)$$

with $a_1 = 1$. In the case of the Kelvin model, $a_1 = -1$ but temperature variation of *sinø* would be the inverse of that indicated by equation 24, an irrational result. Applying equation 24 to the experimental data from the tests conducted by Rowe (1993) on a cantilever trapezoidal beam, the result is:

$$a_0 = 1.181 \times 10^4 \qquad a_1 = -0.3645$$
$$\Delta F = 5.12 \text{ kcal/mol}$$

with the coefficient of determination $r^2 = 0.897$ and the standard error of estimate equal to $s = 0.1422$ for 144 experimental points (from a total of 152). Since $a_1 < 0$ it can be concluded that the Maxwell model is irrealistic for asphalt concrete mixes, while the Kelvin model is more appropriate, at least to the point of describing variation of *sinø* with angular frequency and dynamic modulus. Indeed, a model composed of a dashpot in series with the Kelvin model would be more correct.

Adjustment of Rowe's (1993) data to equation 24 was not the best one possible. The best regression model that was found is given by:

$$\sin\phi = b_0 + b_1 \log_e \omega + b_2 \log_e |E^*| + b_3 \log_e T_{abs} + b_4 VFA \quad (25)$$

where:

$b_0 = -20.05586$ $\quad b_1 = 7.007547 \times 10^{-2}$
$b_2 = -2.899322 \times 10^{-2}$ $\quad b_3 = 3.605885$
$b_4 = -1.237843 \times 10^{-3}$

VFA = voids filled with asphalt (%)

with $r^2 = 0.998$ and $s = 5.3324 \times 10^{-3}$. In this model, ω is the angular frequency (rad/s), $|E^*|$ is the dynamic modulus (MPa) and T_{abs} is the absolute temperature (Kelvin) of the mix. Comparison between predictions made by this model and Rowe's (1993) experimental

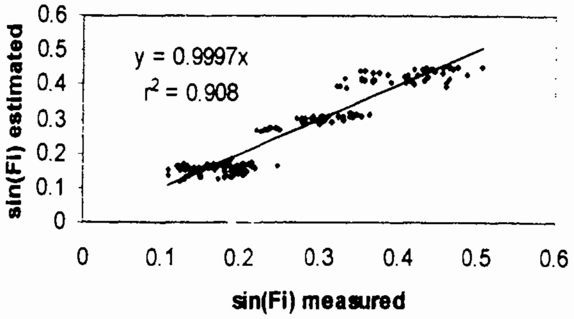

FIGURE 4 Analysis of model for phase angle prediction

data is shown on Figure 4, where it can be seen that the model appears to be reliable for practical application, for the range $4° \leq \phi \leq 40°$.

Employing the Kelvin rheological model, the rate of energy dissipation is given by:

$$\frac{dW_D}{dt} = \sigma\frac{d\varepsilon_{VP}}{dt} = \frac{1}{\eta}\sigma^2 = \frac{\omega}{|E^*|\sin\phi}\sigma^2 \quad (26)$$

Equation (26) refers, however, to the dissipative processes present on a Newtonian fluid, where the strain rate on a creep test is not time dependent, leading to $m = 1$ on equation 10 and, therefore, to $n = 2$ by equation 16. Since fatigue fracture is associated only to a fraction of the total dissipated energy and that $n > 2$ on asphalt concrete, it is necessary to search for a more specific model. It is not important to describe all the dissipative processes occurring under a fatigue test, but only the one that is responsible for the gradual loss of cohesion on the material. Consider now the hypothesis that this part of the dissipative energy could be described by the following expression, written taking equation 26 as a reference:

$$\frac{dW_R}{dt} = -\frac{1}{\eta}\frac{\sigma^n}{W_{R0}^{n-2}} = -\frac{\omega}{|E^*|\sin\phi}\frac{\sigma^n}{W_{R0}^{n-2}} \quad (27)$$

where it is readily apparent that equation 26 is a particular case of equation 27 for $n = 2$. Integrating over the semi-period of tensile stresses on a fatigue sinusoidal test:

$$\frac{dW_R}{dN} = -\frac{1}{\eta}\int_0^{\tau/\omega}\frac{\sigma^n(t)}{W_{R0}^{n-2}}dt \quad (28)$$

It is not possible at this moment to prove that equation 28 is valid, but it can be shown that it is consistent with fatigue test results, if exponent n of that equation is the one observed on fatigue phenomenological laws. Consider now the simple case of a repeated controlled load test where a tensile stress σ_0 is applied during a time Δt_c and the stress pulse is rectangular. In this case, integration of equation 28 for the entire fatigue test will give:

$$\int_{W_{R0}}^{0} W_{R0}^{n-2}dW_R = -\int_0^{N_f}\frac{1}{\eta(N)}\int_0^{\Delta t_c}\sigma_0^n dtdN \quad (29)$$

Integration on equation 29 requires knowledge of the gradual stiffness reduction with number of load cycles on the fatigue test, $|E^*|(N)$. This function will be approximated here by the following expression, derived after observation of some fatigue test results (for example, the ones presented by Rowe, 1993) and referring to the stiffness at the critical point on the test specimen (Figure 5):

$$E(N) = E_0\left[1 - 0.9\left(\frac{N}{N_{f(CT)}}\right)\right] \quad (30)$$

where $N_{f(CT)}$ is the fatigue live at controlled stress tests. This equation assumes that the stiffness at the critical point of the test specimen at failure is equal to 10% of initial value E_0, a condition where a crack is visible at the critical point on the specimen. Equation 30 is represented on Figure 5 by the dotted line.

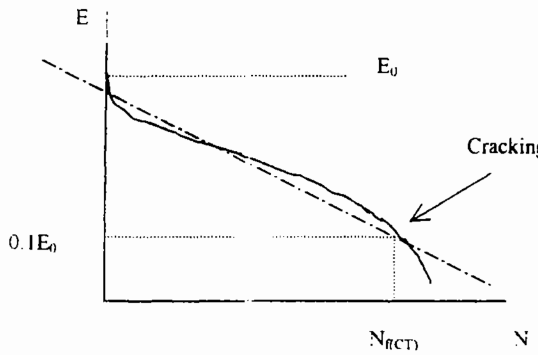

FIGURE 5 Stiffness decrease at controlled stress tests

Employing Rowe's (1993) indication that *sinø* can be considered essentially constant during the fatigue test, in comparison with variation of the dynamic modulus, and employing equation 30, equation 29 becomes:

$$N_f = 6.221 \times 10^{-2}(E_0 \sin\phi)W_{R0}^{n-1}\left(\frac{1}{\sigma_0}\right)^n \quad (31)$$

which is the well known fatigue equation from controlled stress tests. Equation 27 is, therefore, reasonable, if W_{R0} is to be considered a fundamental material property, and would be able not only to describe fatigue cracking under any shape for the applied stress pulse under repeated loads, but also to explain cracking under general loading conditions, such as sustained load (creep) or constant strain rate. If *n* on equation 27 is greater than 2, as is always the case with asphalt concrete under normal service temperatures (when $2 < n < 8$), it is possible to give to the fraction σ^n/W_{R0}^{n-2} the meaning of a "stress-strength ratio" or of an "effective stress", which would be the controlling parameter for the speed of cohesion loss. Equation 27 would, therefore, describe microcracking development until the appearance of a crack of dimensions such that Paris' law becomes applicable.

EXPERIMENTAL INVESTIGATION

In order to apply the proposed model to experimental fatigue data and analyze the associated results, equation 28 will be integrated over the entire fatigue test to give:

$$W_{R0}^{n-1} = \frac{1}{\eta}\int_0^{N_f}\int_0^{\pi/\omega}\sigma^n(t)dtdN = \frac{\omega}{|E^*|_0 \sin\phi_0}\int_0^{N_f}\int_0^{\pi/\omega}\sigma^n(t)dtdN \quad (32)$$

where the viscosity coefficient was assumed to be constant along the fatigue test and equal to its initial value. In spite of the decrease of $|E^*|$ and of the increase of ϕ during the test, this simplifying assumption does not affect the results, due to a compensating effect.

None of the usual fatigue equations can be considered to be a general model for fatigue of asphalt concrete, since exponent of strain amplitude ε_0 is fixed at a constant value on them (n = 4.08 on Rowe's models, n = 5.00 for the Bonnaure et al. models, n = 3.948 for the Tayebali et al. model and n = 3.291 for The Asphalt Institute MS-1 model, for example) while this parameter is known to vary usually between 2.0 and 8.0. In this way, the fatigue law for controlled stress tests given by equations 16, 17 and 18 will be applied here, with parameter *m* being determined from the Van der Poel nomograph with Heukelom and Klomp corrections (Shell, 1978). Controlled strain fatigue test results will not be analyzed here due to the requirement of an exact knowledge of the gradual decrease of the stress amplitude during the test, in order to perform integration on equation 32.

For the simulations here performed, the formula developed by Fonseca (1995) was employed for the dynamic modulus. The flexural stiffness at zero strain and loading frequency of 2 Hz (E_{02}) was estimated by the relation of Witczak and Root (1973), presented by Yoder and Witczak (1975):

$$|E^*| = 0.18089 f^{2.1456} E_{02}^{\left(\frac{14.6918}{f^{0.01}} - 13.5739\right)} \quad (33)$$

and the flexural stiffness at the desired frequency was calculated by:

$$E_0 = E_{02}\frac{|E^*|_f}{|E^*|_{2Hz}} \quad (34)$$

Three loading frequencies (f = 5, 10 and 30 Hz) and four values for the mix temperature (T = 0, 10, 20 and 30°C) were considered, together with all combinations of the following material parameters:

PNT = Penetration of asphalt at 25°C = 45 – 65 – 95 × 10^{-2} cm

V_V = volume of air voids in the mix = 2 – 4 – 6 – 8 %

V_B = asphalt content, in volume = 9 – 12 – 15 – 18 %

and considering only the cases where the volume of voids in the mineral aggregate fell on the range: 75 % < VAM < 85 %. A total of 36 different mixes resulted, since a single gradation curve was adopted for the aggregates, and defined by: P_{200} = 5% (percent passing

N° 200 sieve), $P_{3/8} = 29\%$ (percent retained above sieve 3/8") and $P_4 = 50\%$ (percent retained above N° 4 sieve), with a maximum aggregate diameter of ¾". Ring and Ball softening point was considered dependent on penetration values according to the correlation:

$$T_{RB} = 153.19 \times PNT^{-0.2596} \qquad (35)$$

The phase angle ϕ was calculated by equation 25. The calculated results for W_{R0} and n for some mixes are shown on Table II. Each value of W_{R0} on Table II is the average of 15 points (3 loading frequencies combined with 5 stress amplitudes). The rightmost column shows the average variation of the values of W_{R0} with loading frequency, on the range of frequencies considered (5 to 30 Hz). The W_{R0} values were not dependent upon stress level and the frequency dependence can be judged small.

Table III shows the average values of W_{R0} for each mix, together with the average variation of W_{R0} with temperature. Each line on Table III represents the analysis for 60 points (3 loading frequencies combined with 4 temperatures and 5 stress amplitudes). The rightmost column shows the average variation around the mean value of W_{R0} due to temperature, on the range considered (from 0 to 30°C). It is believed here that the calculated values for W_{R0} were not rigorously temperature insensitive due to the scatter normally found on fatigue tests and which is implicit on equation 18. Parameter W_{R0} would be function only of the asphalt concrete mixture and should not depend upon temperature, since its value would increase only with increases on the amount of heat and of the mechanical effort put on the mixture process. Only for the softest asphalt (PNT = 95) and the lowest temperatures there are significant variations of W_{R0} with temperature.

TABLE II Results for some mixes (V_B = 12%, V_V= 4%)

Mix	*PNT*	*Temperature (°C)*	*n*	*W_{R0} (MPa)*	*Frequency variation (%)*
		0	5.727	4.707	10.5
3	45	10	4.333	5.852	3.7
		20	3.815	5.435	4.4
		30	3.301	4.759	8.7
		0	4.721	6.819	11.5
15	65	10	3.947	6.932	2.5
		20	3.425	6.491	5.7
		30	3.047	4.814	8.9
		0	4.012	10.211	12.4
27	95	10	3.873	6.623	1.8
		20	3.214	6.681	7.0
		30	2.861	4.437	7.9

The calculated values for W_{R0} showed a strong dependency upon volume of asphalt on the mix (V_B) and asphalt penetration (PNT), according to:

$$W_{R0} = 0.01 \times V_B^{0.68}(9.1832 + 2.5244PNT - 0.012174PNT^2) \qquad (36)$$

TABLE III Parameters from the fatigue equation (controlled stress tests)

Mix No.	V_B (%)	V_V (%)	PNT (25°C)	W_{R0} (MPa)	Temperature variation (%)
1	15	2	45	6.133	9.1
2	18	2	45	7.173	9.3
3	12	4	45	5.188	8.8
4	15	4	45	6.064	9.0
5	18	4	45	6.911	9.2
6	9	6	45	4.654	9.1
7	12	6	45	5.362	9.2
8	15	6	45	6.054	9.3
9	18	6	45	6.716	9.4
10	9	8	45	4.761	9.4
11	12	8	45	5.311	9.6
12	15	8	45	5.843	9.7
13	15	2	65	7.580	11.4
14	18	2	65	9.102	11.0
15	12	4	65	6.264	11.6
16	15	4	65	7.554	11.0
17	18	4	65	8.822	10.7
18	9	6	65	5.516	11.5
19	12	6	65	6.572	10.8
20	15	6	65	7.622	10.5
21	18	6	65	8.646	10.3
22	9	8	65	5.739	10.7
23	12	8	65	6.590	10.2
24	15	8	65	7.425	10.0
25	15	2	95	8.640	24.9
26	18	2	95	10.616	26.7
27	12	4	95	6.988	23.1
28	15	4	95	8.668	25.3
29	18	4	95	10.345	27.1
30	9	6	95	6.045	20.7
31	12	6	95	7.408	22.7
32	15	6	95	8.797	24.8
33	18	6	95	10.183	26.8
34	9	8	95	6.366	20.6
35	12	8	95	7.493	22.5
36	15	8	95	8.621	24.5

with $r^2 = 0.942$ and $s = 4.3482 \times 10^{-2}$ for the 36 mixes considered. The strong dependence on V_B is explained by the fact that energy is dissipated only on the binder film and, therefore, there should be a strong relationship between W_{R0} and the amount of asphalt per unit volume of the mix, as also observed by Rowe (1993). The value of W_{R0} should be determined directly from fatigue tests, as was done here, or from other tests (creep, constant strain rate) by application of equation 27. The correlation with an empirical parameter as PNT on equation 36 should be used only for a crude estimate.

The following regression was found to describe the other model parameter:

$$n = 2.5905 \times 10^{11} V_B^{-0.2629} e^{-1.5769 \times 10^{-2} V_V} PNT^{-0.2502} T_{abs}^{-4.0976} \quad (37)$$

($r^2 = 0.967$ $s = 3.4507 \times 10^{-2}$ 144 points)

The rate of loss of the mixture bonding energy under an applied tensile stress is given, as already discussed, by equation 28, for any loading shape $\sigma(t)$. In order to analyze the importance of the time integration of the stress pulse that must be done for application of the model here proposed, the fatigue tests from Raithby and Sterling (1972) will be studied from the viewpoint of this model. Raithby and Sterling (1972) performed fatigue tests in direct tension and in unconfined compression, for several waveforms. Some results, extracted from Tangella et al. (1990), are presented on Table IV.

These results show an increase on the fatigue life with a decrease on the applied initial tensile strain amplitude. The three experimental points lead to the model:

$$N_f = 0.5037 \left(\frac{1}{\varepsilon_0}\right)^{1.2634} \quad (38)$$

with coefficient of determination $r^2 = 0.868$ and standard error of estimate $s = 0.3275$. This model is, however, incompatible with well-established fatigue laws, since the exponent 1.2634 is significantly lower than the exponents usually found, which are greater that 3.0. So, variation of fatigue lives on the tests performed by Raithby and Sterling (1972) cannot be explained solely on the basis of variation of amplitude of applied tensile strain, and the differences on the shapes of the stress pulses are also an important factor.

In order to take into account the different waveforms, the model here developed was applied to these experimental tests. Integrating equation 28, fatigue life is calculated by:

$$N_f = \frac{|E^*| \sin \phi W_{R0}^{n-1} \Delta t_c}{\pi \int_0^{\Delta t_c} \sigma^n(t) dt} \quad (39)$$

Table V shows the calculated fatigue lives with equation 39 and the ones calculated considering the model parameters determined from the fatigue equations 16, 17 and 18 for a mix with $V_B = 12\%$, $V_V = 4\%$, PNT = 65 and a loading frequency of 10 Hz. It is clear from the results that use of the model here developed is meaningful in order to predict relative lives between the three stress shapes, and that direct application of the conventional phenomenological fatigue equations is unable to take into account the effect on the fatigue life of the different shapes of the stress pulses.

TABLE IV Raithby and Sterling (1972) fatigue tests (cyclic axial, on prismatic samples)

Waveform	*Temp. (°C)*	*Stress Amplitude (MPa)*	*Initial Strain Amplitude (10^{-4})*	*Mean Fatigue Life (cycles)*	*Relative Lives*
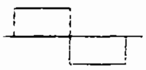	25	0.33	1.7	24690	0.42
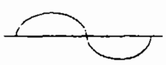	25	0.33	1.2	58950	1.00
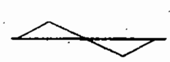	25	0.33	0.67	85570	1.45

TABLE V Analysis of Raithby and Sterling (1972) fatigue tests

Shape of stress pulse	*Experimental (Table IV)*		*Model: equation 39*		*Fatigue equations: 16, 17 and 18*	
	$N_f\,(10^4)$	$N_f/N_{f(sine)}$	$N_f\,(10^6)$	$N_f/N_{f(sine)}$	$N_f\,(10^6)$	$N_f/N_{f(sine)}$
Rectangular	2.469	0.4189	1.6551	0.4110	0.1587	0.3239
Sine	5.895	1.0000	4.0270	1.000	0.4900	1.000
Triangular	8.557	1.4516	7.1599	1.7780	3.2306	6.5933

Raithby and Sterling (1972) performed also fatigue tests in direct tension and compression including stress reversal, and obtained the results presented on Table VI (extracted from Tangella et al. 1990), for a peak stress of 0.76 MPa and temperature at 25°C. They observed that fatigue life is greater if the tensile stress pulse is applied before the compression stress pulse, in comparison with the reverse case. From Table VI, it is clear that the tensile strain pulse has greater duration when the tensile stress is applied after the compression stress pulse, explaining this behaviour. This may be another evidence of the importance of fatigue prediction through stress or strain pulse integration.

TABLE VI Raithby and Sterling (1972) fatigue tests (continued) (loading frequency = 16.7 Hz)

WAVEFORM	*GEOMETRIC MEAN FATIGUE LIFE (CYCLES)*
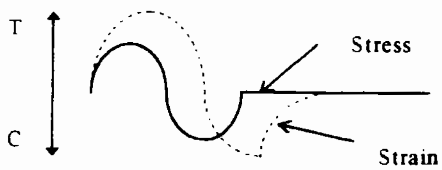	11190
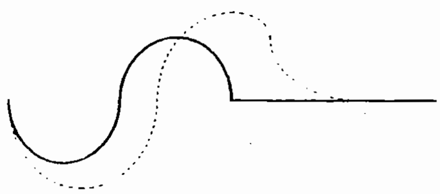	6649
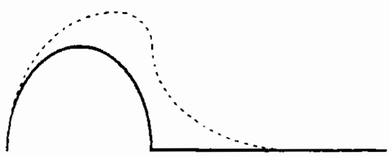	8748
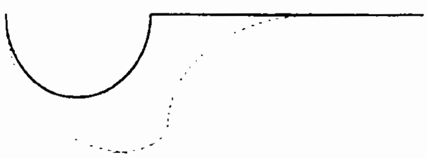	196200

FIELD VALIDATION OF THE PROPOSED MODEL

The damage model here developed will be applied in order to predict the time at which fatigue cracks begin to appear at the pavement surface. Loss of material cohesion under repeated axle loads will be calculated along several paths at the critical plane, defined as the one where loss of cohesion is the largest. Under the passage of an axle load, tensile and shear stresses must be considered, since both have the potential to promote cohesion loss. From the fatigue tests here analysed, only the influence of tensile stresses could be quantified. The effect of the shear stresses (τ) will be accounted for in terms of an equivalent tensile stress:

$$\sigma^* = \rho \times \tau \qquad (40)$$

where ρ is the factor of equivalency, equal to $\rho = 3^{1/2} \approx 1.732$ if the von Mises failure criterion, based on distortion energy density, is applied. Fatigue life under shear stresses, when the shear stresses are generated by unconfined compression, is several times greater than fatigue life under tensile stresses, as indicated on Table VI. Combining equations 7 and 40, the relation between fatigue lives under compressive (N_{fC}) and tensile (N_{fT}) stresses can be given by:

$$\frac{N_{fC}}{N_{fT}} = \left(\frac{\sigma_t}{\sigma^*}\right)^n = \left(\frac{2\sigma_t}{\rho\sigma_c}\right)^n = \left(\frac{2}{\rho}\right)^n \qquad (41)$$

for tensile and compressive pulses of equal magnitude ($\sigma_t = \sigma_c$), since under unconfined compression the maximum shear stress is equal to $\tau = \sigma_c/2$. For $\rho = 3^{1/2} \approx 1.732$, the calculated relation by equation 41 is not consistent with the result from Raithby and Sterling tests (where $N_{fC} / N_{fT} = 22.4$ on Table VI), since even for the greatest possible values of n (≈ 7.0) the calculated relation of fatigue lives by equation 41 would not be greater than 3. Therefore, parameter ρ cannot be given by von Mises failure criterion.

Asphalt concrete is essentially a granular material where the grains are at a high level of interlocking and possessing cohesion due to cementing action of the bituminous binder. Mohr-Coulomb failure criterion seems more adequate in this respect, and leads to:

$$\rho = \frac{2c}{(c + \sigma_n tg\varphi)[\cos\varphi + (1 + \sin\ \varphi)tg\varphi]} \qquad (42)$$

where c is the cohesion intercept, φ is the friction angle and σ_n is the normal stress at the plane where distress is being analysed. This expression was deduced assuming that the tensile stress σ^* equivalent to a shear stress τ is given simply by equating the stress-strength ratios associated with these two parameters, or:

$$\frac{\sigma^*}{\sigma_f} = \frac{\tau}{\tau_f} \qquad (43)$$

where σ_f is the tensile strength and $\tau_f = c + \sigma_n$ tg φ is the shear strength. Estimates of the relation between fatigue lives in compression and in tension applying equation 42 are shown on Table VII for the particular case of $\sigma_n = 0$ and $\varphi = 40°$, where it can be seen that the calculated values are consistent with the experimental one determined by Raithby and Sterling for an exponent of the fatigue law on the order of n = 4, a value commonly found on fatigue tests. Therefore, the indicated relevance of equation 42 reveals the importance of the friction angle of the asphalt concrete mix for its fatigue resistance on the pavement, an aspect that is not evidenced through conventional analyses based on bending fatigue tests and when the effect of shear stresses on the pavement is not taken into account on fatigue damage calculations. Increasing φ will reduce the value of ρ, leading to greater fatigue resistance under the action of shear stresses. The cohesion intercept for practical application of equation 42 can be estimated by the following relation, based on the tensile strength measured on diametral compression tests (σ_R):

$$c = \sigma_R(2\cos\varphi - tg\varphi + 2\cos\varphi \times tg^2\varphi) \qquad (44)$$

TABLE VII Fatigue distress produced by shear stresses

n	N_{fC} / N_{fT} *(von Mises)*	N_{fC} / N_{fT} *(Mohr-Coulomb)*
2	1.33	4.60
3	1.54	9.86
4	1.78	21.15
5	2.05	45.36
6	2.37	97.28
7	2.74	208.61

In order to apply the model here developed to the asphalt concrete layer on the pavement structure, this layer was subdivided on ten sub-layers of equal thickness and damage on sub-layer "i" from an axle load passage along path "j" during environmental conditions "k" will be calculated by:

$$\left(\frac{dW_R}{dN}\right)_{i,j,k} = -\frac{1}{\eta}\int_0^{t_c(\sigma_i)} \frac{\sigma_i^n}{W_{R0}^{n-2}}dt - \frac{1}{\eta}\int_0^{t_c(\tau_i)} \frac{(\rho\tau_i)^n}{W_{R0}^{n-2}}dt \quad (45)$$

where $t_c(\sigma_i)$ and $t_c(\tau_i)$ are the total duration of normal tensile and shear stress pulses, respectively, on sub-layer "i".

Stress pulses were calculated by linear elastic layered theory, with the program FLAPS (Finite Layer Analysis of Pavement Structures), a model based on the process developed by Booker and Small (1985). Stresses calculated by FLAPS program for 8 selected points along the influence area were employed to generate a polynomial interpolation function for the integration on equation 45. Fifth order polynomial interpolation was employed in the integration of the tensile and shear stress pulses along each selected path. Tensile stress for use on equation 45 was calculated from maximum tensile strain by $\sigma = E\varepsilon$, in order to consider the three-dimensional stress state that exists on the pavement structure.

An estimate of the fatigue strength of the pavement along path "j" during environmental conditions "k" can be given by:

$$N_f(i,j,k) = \frac{W_{R0}}{-\left(\frac{dW_R}{dN}\right)_{i,j,k}} \quad (46)$$

If two paths are selected for the analysis, as the ones shown on Figure 6, and the average fatigue strength is calculated from them, the fatigue consumption on each sublayer is given by:

$$c_f(i) = \sum_{K=1}^{N_S} \frac{\Delta N_K}{N_f(i,k)} \quad (47)$$

where N_S is the accumulated number of seasons. This fatigue consumption can be related to a parameter that describe the integrity of the layer or, inversely, the

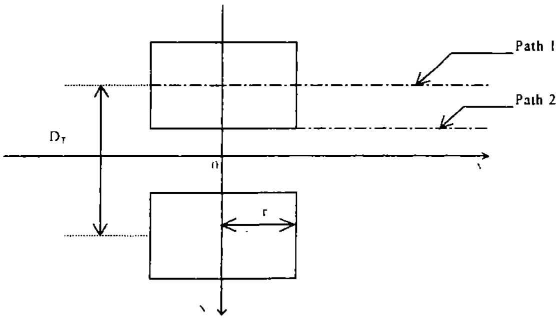

FIGURE 6 Paths selected for damage analvsis

average loss of the mixture bonding energy. For example, the following Integrity Degree index can be employed:

$$ID = \frac{W_R}{W_{R0}} \quad (48)$$

Assuming a linear relation of this index with fatigue consumption, it can be written, for $c_f \leq 1$:

$$ID = 1 - c_f \quad (49)$$

and $ID = 0$ for $c_f > 1$. The Integrity Degree can be related to the degree of cracking of the pavement in order to arrive at a performance prediction model.

This procedure for fatigue life calculation of an asphalt pavement structure has some resemblance with the one applied by Ullidtz (1987) to calculate crack propagation factors for flexible pavements. Raad (1976) also employed successfully the concept of a gradual material deterioration in order to describe fatigue cracking of soil-cement.

The experiment chosen for application of the model was the one conducted by OCDE (1991) at Nantes Circular Test Track. On those accelerated fatigue tests, flexible and semi-rigid pavements were tested under a dual wheel, travelling at speeds ranging from 60.6 to 72.0 km/h. Of importance to the analysis here performed is the behaviour of Structures I and II, both of flexible pavements with a granular base layer (thickness equal to 28 cm) and asphalt concrete thickness shown on Table VIII, together with the number of load repetitions registered at the appearance of the first cracks at the pavement surface. These cracks were transversal to the direction of traffic, indicating a mechanism of fatigue cracking produced by tensile stresses at the bottom of the asphalt concrete surface layer. A dual axle load was employed, with separation distance between wheels equal to 36 cm and wheel contact area equal to 600 cm^2.

The tests were conducted with the asphalt concrete layer experiencing temperatures between 8°C and 24°C. For determination of the pavement layer's elastic moduli, the following response parameters were measured under a moving axle load of 115 kN at 24°C:

D_0 = maximum surface deflection;
ε_x = longitudinal tensile strain under the asphalt concrete layer;
$\varepsilon_z(44)$ = vertical compressive strain at 44 cm below pavement surface;
$\varepsilon_z(64)$ = vertical compressive strain at 64 cm below pavement surface.

Values of the layers' elastic moduli that were found to be more consistent with these instrumentation parameters were:

- For the asphalt concrete layer: E_1 = 5610 MPa;
- For the granular base:
  E_2 = 260 MPa on Section I and on Sector 02 of Section II
  E_2 = 190 MPa on Sector 12 of Section II
- For the granular subgrade soil: E_3 = 58 MPa.

and the comparison between measured and calculated parameters for this set of elastic moduli is shown on Table IX. Some discrepancies are evident and are associated with scatter of the instrumentation results.

The research report presents asphalt concrete parameters referent to the original penetration of the asphalt, which was between 60 and 70. Recovered asphalt at the constructed pavement showed, however, that penetration increased from the original value to a value around 37.5 due to construction hardening effect. This field penetration was employed for the analyses, together with a volume of air voids equal to V_V = 4.4 % (also measured on the pavement) and a volume of asphalt equal to V_B = 13.8 %.

Integration was performed for the entire stress pulse, taking into consideration the traffic speed. Two paths were selected for this analysis, as indicated on Figure 6.

TABLE VIII Pavement structures at Nantes Test Track (OCDE, 1991)

Pavement Section	*Sector No.*	*Axle load (kN)*	*Speed (km/h)*	*Thickness of A.C. layer (cm)*	*N_0 (10^5) Crack appearance*
I	01	115	72.0	6.3	0.726
I	11	100	60.6	6.0	1.030
II	02	115	72.0	13.9	38.000
II	12	100	60.6	13.0	3.700

TABLE IX Calculated and measured response parameters

Pavement Section	*Sector No.*	*D_0 (0.01 mm)*		*ε_x (10^{-4})*		*$\varepsilon_z(44)$ (10^{-3})*		*$\varepsilon_z(64)$ (10^{-3})*	
		Meas.	*Pred.*	*Meas.*	*Pred.*	*Meas.*	*Pred.*	*Meas.*	*Pred.*
I	01	112.0	75.1	1.60	1.60	1.90	0.78	0.50	0.50
I	11	112.0.	75.1	1.60	1.60	1.70	0.78	1.30	0.50
II	02	57.3	56.7	1.25	1.07	1.10	0.54	0.30	0.39
II	12	62.7	61.2	1.40	1.22	1.10	0.58	0.30	0.42

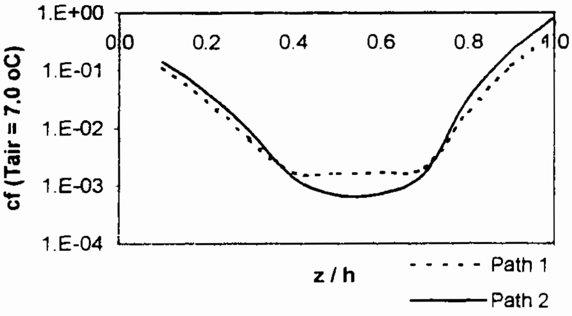

FIGURE 7 Section I – Sector 01 (h_1 = 63 mm)

Performance prediction was made considering the fatigue consumption associated with every month of the test. Mean air temperatures for each month are shown on Table X, and the associated mean monthly temperatures for the asphalt concrete layer were estimated from the following AASHO Road Test model (Gomez and Thompson, 1984):

– For $T_{air} \geq 45.4 + 1.32$ z:

$$T_{\text{mix}} = -10 + 1.39 \times T_{air} - 0.52 \times z \qquad (50)$$

– For $T_{air} < 45.4 + 1.32$ z:

$$T_{\text{mix}} = 7.7 + 1.00 \times T_{air} - 0.004 \times z \qquad (51)$$

where T_{air} and T_{mix} are the mean air and pavement temperatures in °F and z is the depth in inches from the pavement surface at which T_{mix} refers.

TABLE X Conditions on the OCDE (1991) test at Nantes Circular Test Track

Month (1989)	T_{air} *(°C)*	N_{acum} *(10^4) at Section I*		N_{acum} *(10^4) at Section II*	
		Sector 01	*Sector 11*	*Sector 02*	*Sector 12*
February	7.0	3.50	2.55	3.50	2.55
March	8.5	7.26	10.3	10.0	10.6
April	12.0			26.0	25.0
May	12.0			40.0	37.0
June	18.0			68.0	
July	20.0			179.0	
August	22.5			255.0	
September	19.5			344.0	
October	18.0			380.0	

Figures 7 and 8 show the variation of the calculated fatigue consumption along thickness of the asphalt concrete layer, for a certain season, defined by mean air temperature. They indicate that a crack can begin at the top or at the bottom of the asphalt concrete layer. The critical path can be any one of the two paths considered, depending upon pavement structure and temperature. Lateral wandering of the axle load complicates an accurate determination of the critical path. For the analises here performed, the average fatigue consumption of the two selected paths was calculated, as was assumed for writing equation 47.

For the analyses here performed, parameter W_{R0} was calculated from equation 36, parameter n was calculated from equation 37 and parameter $1 / \eta$ was given by the Kelvin model (ω / $|E^*| \sin\phi$), with dynamic modulus being calculated from the Fonseca (1995) equation and $\sin\phi$ being given by equation 25.

Table XI shows the calculated values for the Integrity Degree index at the moment when the first fatigue cracks became apparent at the pavement surface. The average values for the asphalt concrete layer were:

- Section I – sector 01: ID = 0.823
- Section I – sector 11: ID = 0.819
- Section II – sector 12: ID = 0.743
- Section II – sector 02: ID = 0.093

TABLE XI Integrity Degree index for all sections

Sublayer No.	*Section I – 01*	*Section I – 11*	*Section II – 12*	*Section II – 02*
1	0.720	0.666	0.925	0.000
2	0.918	0.900	0.984	0.349
3	0.982	0.978	0.991	0.446
4	0.996	0.996	0.986	0.139
5	0.998	0.998	0.982	0.000
6	0.998	0.998	0.981	0.000
7	0.996	0.996	0.943	0.000
8	0.947	0.953	0.638	0.000
9	0.673	0.708	0.000	0.000
10	0.000	0.000	0.000	0.000
Average ID =	0.823	0.819	0.743	0.093

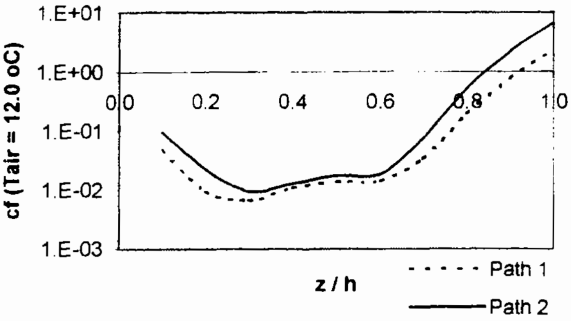

FIGURE 8 Section II – Sector 12 (h_l = 130 mm)

Excluding Section II – sector 02, whose behaviour was strikingly different from the one at Section II – sector 02 of same asphalt concrete thickness, these results show that it could be stablished a critical value of parameter ID (around 0.8) to indicate the appearance of the first fatigue cracks at the pavement surface. The agreement of the calculated values for parameter ID between the first three experimental sections indicates that the model here developed has potential to the development of a reliable performance-predicting tool.

CONCLUSION

Practical implementation of the proposed model needs be addressed in two ways:

(1) For pavement structural design: regressions here developed for calculation of the fundamental mixture parameters (W_{R0}, n and $sin\phi$) could be employed and the model should be applied to the prediction of fatigue cracking observed on in service pavements in order to derive calibration factors. This is being done at the present moment for an extensive data base of highway and airport pavements in Brasil and the use of regressions of equations 36, 37 and 25 is important, since they require only parameters commonly available;

(2) For asphalt concrete mixture design and analysis systems: repeated load or creep tests performed at three temperatures and three loading levels and conducted up to failure can give the fundamental mixture parameters required for the model.

Acknowledgements

To National Council for Scientific and Technological Development of Brasil (CNPq) for the financial support of this research.

References

Molenaar, A.A.A. (1984) Fatigue and reflection cracking due to traffic loads. *Proceedings Association of Asphalt Paving Technologists*, pp. 440–473.

Majidzadeh, K. and Ramsamooj, D.V. (1973) Mechanistic approach to the solution of cracking in pavements. *Highway Research Board*, Special Report 140, pp. 143–157.

Bonnaure, F., Gravois A. and Udron, J. (1980) A new method for predicting the fatigue life of bituminous mixes. *Proceedings Assoctation of Asphalt Paving Technologists*, **49**, pp. 499–529.

Mitchell, J.K. (1976) *Fundamentals of Soil Behaviour*. John Wiley & Sons, New York, p. 292.

Abdel-Hady, M. and Herrin, M. (1966) Characteristics of soil-asphalt as a rate process. *Journal of the Highway Division*, Proc. of the ASCE, **92**, No. HW1, pp. 49–69.

Yoder, E.J. and Witczak, M.W. (1975) *Principles of Pavement Design*. Second Edition, John Wiley & Sons, New York. p. 268.

Tangella, S.C.S.R., Craus. J., Deacon, J.A. and Monismith, C.L. (1990) Summary Report on Fatigue Response of Aspnalt Mixtures. Report TM-UCB-A-003A-89-3 for SHRP Project A-003-A. Institute of Transportation Studies, University of California at Berkeley.

Hertzberg, R.W. (1989) *Detormation and Fracture Mechanics of Engineering Materials*. Third edition, John Wiley & Sons, New York.

Booker, J.R. & Small. J.C. (1985) The Use of Microcomputers to Solve Problems in Geomechanics Using Finite Laver Methods. *Fifth Int. Conf. on Numerical Methods in Geomechanics*, Nagoya, Vol 3.

Fonseca, O.A. (1995) Development of a Time-Dependent Model for the Dynamic Modulus of Asphalt Mixes. PhD Thesis, University of Maryland.

Rowe, G.M. (1993) Performance of Asphalt Mixtures in the Trapezoidal Fatigue Test. *Journal of the Association of Asphalt Paving Technologists*, **62**, pp. 344 – 384.

Tayebali, A.A., Deacon, J.A., Coplantz, J.S. and Monismith, C.L. (1993) Modelling Fatigue Response of Asphalt-Aggregate Mixtures. *Journal of the Association of Asphalt Paving Technologists*, **62**, pp. 385 – 421.

Ullidtz, P. (1987) *Pavement Analysis*. Elsevier, Amsterdam.

Raad, L. (1976) Design Criteria for Soil-Cement Bases. PhD Thesis, University of California at Berkeley.

Maupin, G.W. and Freeman Jr., J.R. (1976) Simple procedure for fatigue characterization of bituminous concrete. Report No. FHWA-RD-76-102, Virginia Highway and Transportation Research Council, University Station, Virginia.

Folias, E.S. (1970) On a plate supported by an elastic foundation and containing a finite crack. *Int. Journal of Fracture Mechanics*, **6**, No. 3, September, pp. 257–263.

Gomez. M. and Thompson, R. (1984) Mechanistic Design Concepts for Full-Depth Asphalt Concrete Pavements. Report No.

FHWA-IL-UI-207, University of Illinois at Urbana-Champaign.

OCDE (1991) *Essai OCDE en vraie grandeur des superstructures routières. Recherche en matiere de routes et de transports routiers*. DIRR N° 125145, Paris, France.

Shell International Petroleum Company Ltd. (1978), *Shell Pavement Design Manual*. London.

Jayawickrama, P.W. and Lytton, R.L. (1987) Methodology for predicting asphalt concrete overlay life against reflection cracking. *Sixth Int. Conf. on Structural Design of Asphalt Pavements*, University of Michigan, pp. 912–924.

Phadnavis, D.G. and Swaminathan, C.G. (1977) The response of a bituminous mixture at failure to different loading conditions. *Proc. Australian Road Research*, **7**. No. 2, June, pp. 23–31.